doi:10.1093/brain/awr357 Brain 2012: 135; 469–482 | 469

BRAIN
A JOURNAL OF NEUROLOGY

Cobblestone lissencephaly: neuropathological subtypes and correlations with genes of dystroglycanopathies

Louise Devisme,[1] Céline Bouchet,[2] Marie Gonzalès,[3] Elisabeth Alanio,[4] Anne Bazin,[5] Bettina Bessières,[6] Nicole Bigi,[7] Patricia Blanchet,[7] Dominique Bonneau,[8] Maryse Bonnières,[6] Martine Bucourt,[9] Dominique Carles,[10] Bénedicte Clarisse,[11] Sophie Delahaye,[12] Catherine Fallet-Bianco,[13] Dominique Figarella-Branger,[14] Dominique Gaillard,[4] Bernard Gasser,[15] Anne-Lise Delezoide,[16] Fabien Guimiot,[16] Madeleine Joubert,[17] Nicole Laurent,[18] Annie Laquerrière,[19] Agnès Liprandi,[14] Philippe Loget,[20] Pascale Marcorelles,[21] Jelena Martinovic,[5,6] Francoise Menez,[16] Sophie Patrier,[3] Fanny Pelluard,[10] Marie-José Perez,[7] Caroline Rouleau,[22] Stéphane Triau,[23] Tania Attié-Bitach,[6] Sandrine Vuillaumier-Barrot,[2] Nathalie Seta[2] and Férechté Encha-Razavi[6]

1 Institut de Pathologie, Centre de Biologie-Pathologie, CHU Lille, 33.3.20446983, France
2 The Assistance Publique-Hôpitaux de Paris (APHP), Hôpital Bichat-Claude Bernard, Biochimie, Paris, 33.1.40258541, France
3 The Assistance Publique-Hôpitaux de Paris (APHP), Hôpital Armand Trousseau, Génétique et Embryologie Médicales, Université Pierre et Marie Curie, Paris, 33.1.44735488, France
4 Génétique, Laboratoire Pol Bouin, CHU Reims, 33.3.26787878, France
5 Laboratoire Pasteur-Cerba, Pontoise, 33.1.34402112, France
6 The Assistance Publique-Hôpitaux de Paris (APHP), Hôpital Necker-Enfants Malades, Histologie-Embryologie-Cytogénétique, 33.1.44494984, France
7 Génétique Médicale, CHRU A de Villeneuve, Montpellier, 33.4.67336564, France
8 Génétique Médicale, CHU Angers, Université d'Angers, Inserm U694, 33.2.41353883, France
9 The Assistance Publique-Hôpitaux de Paris (APHP), Hôpital Jean Verdier, Anatomie et Cytologie Pathologiques, Bondy, 33.1.48026669, France
10 Anatomie et Cytologie Pathologiques, Hôpital Pellegrin, Université Victor Segalen - Bordeaux 2 Bordeaux, 33.5.56799823, France
11 Université Paris Descartes, Santé Publique et Environnement, Paris, 33.1.53739726, France
12 The Assistance Publique-Hôpitaux de Paris (APHP), Hôpital Armand Trousseau, Diagnostic Prénatal, Paris, 33.1.44494030, France
13 Neuropathologie, Hôpital Sainte Anne, Paris, 33.1.45658659, France
14 Assistance Publique-Hopitaux de Marseille (APHM), Hôpital de La Timone, Anatomie Pathologique et Neuropathologie, Université de la Méditerranée, Marseille, 33.4.91385528, France
15 Pathologie, Hôpital E Muller, Mulhouse, 33.3.89648725, France
16 The Assistance Publique-Hôpitaux de Paris (APHP), Hôpital Robert Debré, Biologie du Développement, Université Paris Diderot, Paris, 33.1.40032338, France
17 Anatomie Pathologique, CHU Hôtel Dieu, Nantes, 33.2.40087402, France
18 Anatomie Pathologique, CHU Dijon, 33.3.80393345, France
19 Anatomie et Cytologie Pathologiques, Hôpital Charles Nicolle, Université de Rouen, CHU-Rouen, 33.2.32880362, France
20 Anatomie Pathologique, CHU Pontchaillou, Rennes, 33.2.99284279, France
21 Anatomie Pathologique, CHU Brest, 33.2. 98223217, France
22 Anatomie Pathologique, CHU Montpellier, Université 33.4.67337283, France
23 Département de Pathologie Cellulaire et Tissulaire, CHU Angers, 33.2.41354169 France

Received August 5, 2011. Revised October 28, 2011. Accepted November 23, 2011

Correspondence to: Dr F. Encha-Razavi,
Service Histologie-Embryologie,
Hôpital Necker-Enfants malades,
149 rue de Sèvres,
Paris 75015, France
E-mail: ferechte.razavi@nck.aphp.fr

Cobblestone lissencephaly represents a peculiar brain malformation with characteristic radiological anomalies, defined as cortical dysplasia combined with dysmyelination, dysplastic cerebellum with cysts and brainstem hypoplasia. Cortical dysplasia results from neuroglial overmigration into the arachnoid space, forming an extracortical layer, responsible for agyria and/or 'cobblestone' brain surface and ventricular enlargement. The underlying mechanism is a disruption of the glia limitans, the outermost layer of the brain. Cobblestone lissencephaly is pathognomonic of a continuum of autosomal recessive diseases with cerebral, ocular and muscular deficits, Walker–Warburg syndrome, muscle–eye–brain and Fukuyama muscular dystrophy. Mutations in *POMT1*, *POMT2*, *POMGNT1*, *LARGE*, *FKTN* and *FKRP* genes attributed these diseases to α-dystroglycanopathies. However, studies have not been able to identify causal mutations in the majority of patients and to establish a clear phenotype/genotype correlation. Therefore, we decided to perform a detailed neuropathological survey and molecular screenings in 65 foetal cases selected on the basis of histopathological criteria. After sequencing the six genes of α-dystroglycanopathies, a causal mutation was observed in 66% of cases. On the basis of a ratio of severity, three subtypes clearly emerged. The most severe, which we called cobblestone lissencephaly A, was linked to mutations in *POMT1* (34%), *POMT2* (8%) and *FKRP* (1.5%). The least severe, cobblestone lissencephaly C, was linked to *POMGNT1* mutations (18%). An intermediary type, cobblestone lissencephaly B, was linked to *LARGE* mutations (4.5%) identified for the first time in foetuses. We conclude that cobblestone lissencephaly encompasses three distinct subtypes of cortical malformations with different degrees of neuroglial ectopia into the arachnoid space and cortical plate disorganization regardless of gestational age. In the cerebellum, histopathological changes support the novel hypothesis that abnormal lamination arises from a deficiency in granule cells. Our studies demonstrate the positive impact of histoneuropathology on the identification of α-dystroglycanopathies found in 66% of cases, while with neuroimaging criteria and biological values, mutations are found in 32–50% of patients. Interestingly, our morphological classification was central in the orientation of genetic screening of *POMT1*, *POMT2*, *POMGNT1*, *LARGE* and *FKRP*. Despite intensive research, one-third of our cases remained unexplained; suggesting that other genes and/or pathways may be involved. This material offers a rich resource for studies on the affected neurodevelopmental processes of cobblestone lissencephaly and on the identification of other responsible gene(s)/pathway(s).

Keywords: cobblestone lissencephaly; lissencephaly type II; α-dystroglycanopathies; Walker–Warburg syndrome; muscle–eye–brain disease

Abbreviations: MDDGA = muscular congenital α-dystroglycanopathy with brain and eye anomalies; OMIM = Online Mendelian Inheritance in Man

Introduction

Cobblestone lissencephaly represents a peculiar brain malformation with characteristic radiological anomalies defined as cerebral cortical dysplasia with irregular limit between white and grey matter, dysmyelination, severe dysplastic cerebellum with cysts and brainstem hypoplasia (van der Knaap *et al.*, 1997; Barkovich, 1998; Jissendi-Tchofo *et al.*, 2009). Cortical malformations are due to neuroglial overmigration into the arachnoid space resulting in the formation of an extracortical neuroglial layer responsible for agyria and/or irregular, 'cobblestone', surface of the brain and ventriculomegaly. This distinct form of lissencephaly was reported by Pagon *et al*. (1978) and opposed by Dambska *et al.* (1983) to the 'four layered' lissencephaly, described by Jellinger and Rett (1976). The classical form therefore was recognized as lissencephaly type I and linked to a primitive neuronal migration failure. In contrast, the second type called lissencephaly type II, was attributed to a defect of the outermost pial–glial layer of the brain, resulting in abnormal settlement of the cortical plate (Nakano *et al.*, 1996). In each type, neuropathological studies and molecular screenings demonstrated morphological diversity and genetic heterogeneity (Viot *et al.*, 2004; Encha-Razavi and Chelly, 2006). This led to the reclassification of lissencephaly type I and type II as 'classical' and 'cobblestone' lissencephaly, respectively (Barkovich *et al.*, 2001).

Cobblestone lissencephaly is considered to be pathognomonic of a continuum of recessive autosomal disorders with ocular and muscular deficits, called Walker–Warburg syndrome, muscle–eye–brain Disease and Fukuyama muscular and cerebral dystrophy. The Walker–Warburg syndrome (OMIM #236670), also known under HARD + / – E eponym (hydrocephalus, agyria, retinal dysplasia, encephalocele) is characterized by major neurological deficit, visual and muscular impairment and a rapid fatal outcome (Dobyns *et al.*, 1989). Less severe within the same spectrum, with

subtle eye abnormalities, less significant neurological deficit and a milder muscular dystrophy is muscle–eye–brain disease (Santavuori *et al.*, 1989), first described in a Finnish population (OMIM #253280); and Fukuyama muscular and cerebral dystrophy, common in Japan (OMIM #253800) (Fukuyama *et al.*, 1981).

Classically these syndromes, with cerebral ocular and muscular dystrophy, are attributed to abnormal glycosylation of α-dystroglycan, and are now designated 'muscular congenital α-dystroglycanopathy with brain and eye anomalies' (MDDGA, OMIM #253800). α-Dystroglycan is a complex molecule involved in a broad range of biological processes (Barresi and Campbell, 2006; Chan *et al.*, 2010). Its aberrant post-translational modification is associated with mutations in at least six genes (*POMT1*, *POMT2*, *POMGNT1*, *LARGE*, *FKTN* and *FKRP*) (van Reeuwijk *et al.*, 2005; Godfrey *et al.*, 2007; Clement *et al.*, 2008). Mutations in one of these genes are found in 32–50% of patients (Godfrey *et al.*, 2007; Mercuri *et al.*, 2009). Despite intensive research, studies have not been able to identify causal mutations in the majority of patients and to establish a clear phenotype/genotype correlation to account for phenotypic variations (Godfrey *et al.*, 2007; Mercuri *et al.*, 2009). This could be improved by a better knowledge of neurohistopathological changes, which are rarely available. Indeed in most reports, brains anomalies are documented on the basis of neuroimaging findings alone. Therefore, we decided to report on neuropathological data and on genotype/phenotype correlations in a series of 65 foetal cases selected on the basis of histoneuropathological criteria.

During post-natal life, clinical variations make diagnosis of MDDGA uncertain. Diagnosis of cobblestone lissencephaly relies on neuroimaging screening (Jissendi-Tchofo *et al.*, 2009). The creatine phosphokinase values and muscular anomalies point to α-dystroglycanopathies. Diagnosis of prenatal forms may be challenging too. In foetuses, despite performances of prenatal brain imaging, agyria/pachygyria could not be discussed before 22 weeks gestation because cerebral hemispheres are smooth until 20 weeks gestation. In addition, muscular dystrophy could not be demonstrated because of lack of creatine phosphokinase value controls and skeletal muscle immaturity. Ventricular enlargement with abnormal cerebral mantle lamination and brainstem and cerebellum anomalies may orient the diagnosis (Barkovich *et al.*, 2005). However, confirmation of the cobblestone lissencephaly relies on the histological identification of the characteristic cortical malformation made of neuroglial ectopia into the arachnoid space, and loss of cortical plate lamination, associated to brainstem and cerebellar dysplasia. In our series, after sequencing the six genes involved in α-dystroglycanopathy, we observed a causal mutation in 66% of cases (68% of families). To identify phenotypic variations, we considered the spectrum of cerebral, cerebellar and ocular anomalies in relation to gestational age. This permitted definition of a scoring system of histoneuropathological severity and identification of three distinct groups with good genetic correlation. In cobblestone lisssencephaly, neuropathological findings appear to be instrumental in the identification of α-dystroglycanopathies and in molecular screening orientation. In addition, they permit a better characterization and understanding of the neurodevelopmental processes underlying supratentorial and infratentorial anomalies.

Materials and methods

Population and techniques

This morphological and molecular study of cobblestone lissencephaly was performed on archival material derived from 19 French embryo–foetal pathology centres. In a previous molecular study, we performed sequencing of the six major genes of α-dystroglycanopathy in 47 cases (Bouchet *et al.*, 2007). In this study, we expanded the series to 65 cases (foetuses and neonates) (27 females/38 males), ranging between 14 and 41 weeks gestation and including 47 cases aged between 21 and 28 weeks gestation. They were born to 53 families, mainly from French extraction. Consanguinity was acknowledged in eight families. Pregnancies were terminated according to the French legislation for severe cerebral malformations. In index cases, brain anomalies were detected on routine ultrasound examination during the second quarter of pregnancy. MRI was not performed. Recurrences were diagnosed on ultrasound as soon as 14 weeks gestation. In index cases, brain anomalies include ventricular enlargement, isolated or associated with abnormal gyration and cerebellar anomalies. Cerebellum was described as cystic or with a Dandy–Walker malformation appearance. Other brain abnormalities such as agenesis of corpus callosum and holoprosencephaly were noticed occasionally. In all index cases, diagnosis of cobblestone lissencephaly was histological. Post-mortem examination was performed after parental consent and included external examination, X-rays, photographs, macroscopic and histological examination of viscera and neuropathological analysis. Frozen tissues were conserved. Paraffin sections of skeletal muscle stained with haematoxylin and eosin were available in all cases.

Neuropathological study and scoring

Neuropathological re-evaluation was performed by two experts in neurodevelopment, on specimens sampled from the supra and infratentorial levels, stained with haematoxylin and eosin and/or cresyl violet. At the supratentorial level, specimens were sampled from frontal, parietal, temporal and occipital regions. Infratentorial specimens included transverse sections of the mesencephalon (cerebral peduncles) and sagittal and/or transverse sections of the pons and the cerebellum and the medulla oblongata. Eye sections, stained with haematoxylin and eosin, were available in 44 cases.

For inclusion criteria of cobblestone lissencephaly we retained the minimal association of (i) neuroglial ectopia within the arachnoid space; (ii) abnormal cortical lamination; and (iii) brainstem and cerebellar dysplasia. Careful analysis of the cortical and cerebellar phenotypes revealed phenotypic variations. We hypothesized that at the supratentorial level, the thickness of the extracortical layer may predict the severity of neuroglial ectopia and the abnormal cortical lamination thereof. The characteristic layering of the cerebral mantle (cortex, subplate, intermediate zone, subventricular/ventricular zone) seen in normal brains of 20–24 weeks gestation is not recognizable in cobblestone lissencephaly. Conversely, the interface between the extracortical layer and the residual cortical plate is marked by deepened arachnoidal vessels with tangential orientation (perpendicular to perforating cortical vessels). The inferior limit of the residual cortex (mainly cellular) corresponds to the borderline with the intermediary zone (mostly fibrillar). Measurements of the extracortical layer and the residual cortical plate were performed on the neocortices at the frontoparietal level, using an ocular micrometer. To address the question whether the severity of brain anomalies was related to the maturity of the foetus, the extracortical layer/cortical plate ratio was evaluated

considering gestational age. The thickness of the body of the corpus callosum was measured on the histological preparations considering the gestational age. Compared to the 'normal' average of 2 mm at mid-gestation, the corpus callosum was considered as thin when <2 mm or thick when >2 mm.

Molecular study

Molecular screening was performed on genomic DNA and on complementary DNA extracted from frozen foetal tissues, according to standard protocols (Bouchet *et al.*, 2007). Preliminary studies of allelic transmission were performed using microsatellites analysis in consanguineous and multiplex families. The six genes (*POMT1*, *POMT2*, *POMGnT1*, *FKTN*, *FKRP* and *LARGE)* were studied by direct genomic DNA and/or complementary DNA sequencing. In mutated cases, autosomal recessive transmission was confirmed after parental molecular screening. Each unknown missense variation was examined in at least 100 control individuals and tested *in silico* using different software to evaluate the predicted effect on protein activity (Bouchet *et al.*, 2007). Splicing mutations were confirmed after complementary DNA studies and large rearrangements were studied using either fluorescent quantitative polymerase chain reaction and/or comparative genomic hybridization array (Agilent Technologies). Genomic DNA and complementary DNA primers for sequencing and probes design for quantitative polymerase chain reaction and comparative genomic hybridization arrays are available upon request.

Results

Clinicopathological classification

External and/or visceral malformations, isolated or in association, were found in 50/65 foetuses (77%) and are listed in Table 1. Paraffin sections of skeletal muscles stained with haematoxylin and eosin did not show significant changes in routine histology.

Concerning the CNS anomalies, expressivity was variable (Table 2). Cerebral hemispheres were usually enlarged, covered with adherent and opalescent meninges, containing fine tortuous vessels (Fig. 1A–C). Between 18 and 22 weeks gestation, insular lobe operculization was delayed (Fig. 1A). On coronal sections, tetraventricular dilatation was constant. The corpus callosum was either normal, thin, thick or absent. Interestingly, histological study observed a correlation between the thickness of the extracortical layer and the underlying cortical plate. Severe neuroglial ectopia results in the obliteration of the arachnoidal space by a thick densely cellular extracortical layer, and the reduction and abnormal lamination of the underlying cortical plate (Fig. 2A). In these cases, the thickness of the extracortical layer was greater than the residual cortical plate and the extracortical layer/cortical plate ratio was therefore positive (>1) (Fig. 2C). Conversely, when the neuroglial ectopia was milder, the extracortical layer was thinner than the cortical plate and the extracortical layer/cortical plate ratio was negative ($\leqslant 1$) (Fig. 2B and D).

Supratentorial anomalies are detailed below within each subtype. The extracortical layer/cortical plate ratio, as well as the corpus callosum anomalies were independent of gestational age.

The brainstem was affected in all cases and at all examined levels (cerebral peduncles, pons, medulla). Cerebral peduncles surrounded by thick and adherent leptomeninges were hypoplastic (Fig. 3A). Longitudinal tracts were drastically reduced. Numerous tracts were found in an ectopic location within the arachnoid space (Fig. 3B and C). The aqueduct of Sylvius was dysmorphic, either dilated or narrowed (Fig. 3B). The pons was shortened and flattened surrounded by thick meninges (Fig. 3D–F). A 'Z' shape deviation at the midbrain–hindbrain boundary could be seen on sagittal sections of the brainstem in some cases (Fig. 3E and F). In one case, the pons was split by a midline longitudinal fissure in two longitudinal columns, containing chaotic tracts (Fig. 3D). Cranial nerve nuclei were present but displaced. In the pons, the tegmentum was hypoplastic and the pontine nuclei and tracts were drastically reduced. The arachnoidal space was filled with ectopic neurons and fibres. In the medulla, pyramids were hypoplastic or absent. The olivary complex was pachygyric.

Brainstem anomalies displayed similar patterns of severity, while cerebellar changes were of variable expressivity in terms of distribution (diffuse to focal) and severity (major to minor). Diffuse forms affecting cerebellar hemispheres and the vermis could be opposed to focal forms restricted to some folia. In both forms, cerebellar dysplasia could be major or minor. Major forms were characterized by a severe dysplasia affecting the cerebellar hemispheres and the vermis (Fig. 3G). Folia showed a chaotic organization; they were fused and displayed a characteristic 'lacunar' organization (Fig. 3H). Lacunas were formed by a 'core' of arachnoidal tissue, either surrounded by irregular rims of granule cells and/or Purkinje cells or devoid of any laminar organization (Fig. 3H). Careful histological analysis showed ectopic clusters of granule cells spanned in the entire pericerebellar arachnoid, including the vermis and the cerebellar hemispheres. Under the arachnoid, the external granular layer was poorly cellular, fragmented or devoid of granule cells (Fig. 3H). The Purkinje cells were often misoriented. Minor forms were reduced to focal nests of granule cells in the arachnoid space (Fig. 3I).

Retinal dysplasia varied from focal to diffuse and from major to minor, ranging from total lack of lamination to foci of dysplasia. Our scoring system, based on the extracortical layer/cortical plate ratio, allowed us to define three distinct phenotypes, that we called cobblestone lissencephaly A, cobblestone lissencephaly B and cobblestone lissencephaly C, respectively.

Cobblestone lissencephaly A

This group concerned 48/65 cases (74%). Aged from 14 to 41 weeks gestation, they all displayed a positive extracortical layer/cortical plate ratio. On coronal sections, severe tetraventricular dilatation was constant. The corpus callosum was evaluable in 37 cases. It was absent in 16 cases, abnormally thin in 15 cases (from 18 to 37 weeks gestation) and thick in six cases (from 19 to 26 weeks gestation). At the microscopic level, the arachnoid space was filled by massive and diffuse neuroglial ectopia found all around the cerebral hemispheres (Fig. 2A). Consequently, the residual cortical plate was reduced to a thin rim or foci of scattered neuroblasts. The interface between the extracortical layer and the cortical plate was virtual and demarcated by large arachnoidal vessels (Fig. 2C). In the dorsomedial telencephalon, neuroglial ectopia resulted in the interdigitation of the opposite cortical

Table 1 External and visceral malformations in the series of 65 cases with foetal cobblestone lissencephaly (53 families)

Families	*n*	Sex	Weeks gestation	Gene mutated	NTD	Limb deformations	External eyes anomalies	Facial cleft	Micropenis	Gonadal dysgenesis	Visceral malformations
F1	1	F	24		+	–	–	–	–	–	Kidney
	2	M	17		–	–	–	–	–	–	Digestive
	3	F	18		+	–	–	–	–	+	–
F2	4	F	19		+	–	–	–	–	–	–
F3	5	F	26	*POMT1*	–	–	+	–	–	–	–
F4	6	M	36	*POMT1*	+	+	+	–	+	+	–
F5	7	M	25		+	–	+	–	–	+	Heart
F6	8	M	23		+	+	–	–	–	–	–
F7	9	M	28		+	+	+	–	+	–	Heart
F8	10	M	21	*POMT1*	+	–	+	–	–	+	–
F9	11	M	20	*POMT1*	–	–	–	+	–	–	–
	12	M	14	*POMT1*	+	–	–	–	–	+	–
	13	M	15	*POMT1*	–	–	–	+	+	–	–
F10	14	M	20	*POMT1*	+	–	–	+	+	–	Kidney
F11	15	M	20	*POMGNT1*	–	–	–	–	–	–	–
	16	F	18	*POMGNT1*	–	–	–	–	–	–	–
F12	17	M	20	*POMGNT1*	–	+	–	–	–	–	–
F13	18	F	23	*POMT1*	–	–	–	+	–	+	–
	19	F	21	*POMT1*	–	+	+	–	–	–	–
F14	20	M	24	*POMGNT1*	–	–	–	–	–	–	–
F15	21	M	18		–	–	–	–	–	–	Kidney
F16	22	F	23		–	–	–	–	–	–	–
F17	23	F	25		–	–	–	–	–	–	–
F18	24	M	23	*POMGNT1*	–	+	–	–	–	–	–
F19	25	F	24	*FKRP*	–	–	–	–	–	–	Digestive
F20	26	F	24		–	+	–	–	–	–	Pulmonary
F21	27	M	27	*LARGE*	–	–	+	–	–	–	–
F22	28	F	41	*POMT1*	–	–	+	+	–	–	–
F23	29	M	16		–	–	–	–	–	–	–
	30	F	19		–	+	–	–	–	–	–
F24	31	M	23		+	–	–	–	–	–	Kidney Digestive
	32	F	23		+	–	–	–	–	–	–
	33	M	17		+	+	+	–	–	–	–
F25	34	F	24		–	+	–	–	–	–	–
F26	35	M	24		+	–	–	–	–	–	–
F27	36	M	23		–	–	–	–	–	–	Kidney
F28	37	M	28	*POMT2*	–	+	–	–	+	+	–
F29	38	M	22	*POMT1*	–	–	–	–	–	–	–
F30	39	M	37		+	–	+	–	–	–	Pulmonary
F31	40	F	19	*POMT1*	–	–	–	–	–	–	–
F32	41	F	26	*POMGNT1*	–	+	–	–	–	–	–
F33	42	F	23	*POMT1*	–	–	–	–	–	–	–
F34	43	M	20	*POMT1*	–	–	–	–	–	–	Kidney
F35	44	M	32	*POMGNT1*	–	–	–	–	–	–	–
F36	45	F	24	*POMT1*	+	–	+	–	–	–	Kidney
	46	F	20	*POMT1*	–	–	–	–	–	–	Thymus
F37	47	F	24	*POMT1*	–	–	–	–	–	–	Kidney
F38	48	F	31	*POMT1*	–	+	–	–	–	–	Kidney, Heart Pulmonary
F39	49	M	26	*POMT2*	–	–	–	–	–	+	Heart
F40	50	M	22	*POMT2*	–	–	–	–	–	+	Kidney
F41	51	M	23	*POMGNT1*	–	–	–	–	–	–	–
F42	52	F	21	*POMGNT1*	–	–	–	–	–	–	–
	53	M	22	*POMGNT1*	–	–	–	–	–	–	–
F43	54	M	27	*POMT1*	–	–	+	–	–	+	Kidney Pulmonary
F44	55	M	24	*POMGNT1*	–	+	+	–	–	–	–

(continued)

Table 1 Continued

Families	*n*	Sex	Weeks gestation	Gene mutated	NTD	Limb deformations	External eyes anomalies	Facial cleft	Micropenis	Gonadal dysgenesis	Visceral malformations
F45	56	F	25	*POMT1*	+	–	–	–	–	–	Kidney Digestive
F46	57	F	23	*POMT1*	–	–	–	+	–	–	Kidney
F47	58	M	22	*LARGE*	–	–	–	–	–	–	–
	59	F	23	*LARGE*	–	–	–	–	–	–	–
F48	60	M	15	*POMT2*	–	–	–	–	–	–	Kidney
F49	61	M	27	*POMT2*	+	–	–	–	–	–	Kidney, Heart
F50	62	M	25		+	+	–	–	–	–	Kidney
F51	63	M	24		–	–	–	–	+	+	–
F52	64	F	23	*POMT1*	–	–	+	–	–	–	–
F53	65	M	24	*POMGNT1*	–	+	–	–	–	–	–

F = female; M = male; + = present; – = absent; NTD = neural tube defect.

Table 2 Neuropathological findings in the series of 65 cases with foetal cobblestone lissencephaly (53 families)

Families	Cases	Weeks gestation	Mutation	Extracortical layer/cortical plate			Cerebellar dysplasia				Retinal dysplasia			
							Extension		Severity		Extension		Severity	
				Positive	Variable	Negative	Diffuse	Focal	Major	Minor	Diffuse	Focal	Major	Minor
F1	1	24		+			+			+	NA	NA	NA	NA
	2	17		+			+			+	+			+
	3	18		+			+			+	+			+
F2	4	19		+			+		+		+			+
F3	5	26	*POMT1*	+			+		+		NA	NA	NA	NA
F4	6	36	*POMT1*	+			+		+		NA	NA	NA	NA
F5	7	25		+			+		+		NA	NA	NA	NA
F6	8	23		+			+			+	+			+
F7	9	28		+			+		+	+	+			
F8	10	21	*POMT1*	+			+		+	+	+			
F9	11	20	*POMT1*	+			+		+		+		+	
	12	14	*POMT1*	+			+		+		+		+	
	13	15	*POMT1*	+			+		+		+		+	
F10	14	20	*POMT1*	+			+			+	NA	NA	NA	NA
F11	15	20	*POMGNT1*			+	+			+	NA	NA	NA	NA
	16	18	*POMGNT1*			+	+			+	0	0	0	0
F12	17	20	*POMGNT1*			+	+			+	NA	NA	NA	NA
F13	18	23	*POMT1*	+			+		+		+			+
	19	21	*POMT1*	+			+		+			+		+
F14	20	24	*POMGNT1*			+		+		+		+		+
F15	21	18		+			+		+		0	0	0	0
F16	22	23				+		+		+	NA	NA	NA	NA
F17	23	25			+		+		+		NA	NA	NA	NA
F18	24	23	*POMGNT1*			+		+		+		+		+
F19	25	24	*FKRP*	+			+			+	+			+
F20	26	24		+			+		+		+		+	
F21	27	27	*LARGE*		+		+		+		NA	NA	NA	NA
F22	28	41	*POMT1*	+			+		+		+			+
F23	29	16		+			+			+	+			+
	30	19		+			+			+	NA	NA	NA	NA
F24	31	23		+			+		+		+		+	
	32	23		+			+				+	+		+
	33	17		+			+			+		+		+
F25	34	24		+			+		+		+		+	

(continued)

Table 2 Continued

Families	Cases	Weeks gestation	Mutation	Extracortical layer/cortical plate			Cerebellar dysplasia				Retinal dysplasia			
							Extension		Severity		Extension		Severity	
				Positive	Variable	Negative	Diffuse	Focal	Major	Minor	Diffuse	Focal	Major	Minor
F26	35	24		+			+		+		+		+	
F27	36	23		+			+		+		+			+
F28	37	28	*POMT2*	+			+		+		NA	NA	NA	NA
F29	38	22	*POMT1*	+			+		+		NA	NA	NA	NA
F30	39	37		+			+		+		0	0	0	0
F31	40	19	*POMT1*	+			+		+		+		+	
F32	41	26	*POMGNT1*			+	+				NA	NA	NA	NA
F33	42	23	*POMT1*	+			+		+		+			+
F34	43	20	*POMT1*	+			+		+		+			+
F35	44	32	*POMGNT1*			+		+	+		NA	NA	NA	NA
F36	45	24	*POMT1*	+			+		+		+			+
	46	20	*POMT1*	+			+		+		NA	NA	NA	NA
F37	47	24	*POMT1*	+			+		+		NA	NA	NA	NA
F38	48	31	*POMT1*	+			+		+		+			+
F39	49	26	*POMT2*	+			+		+		+		+	
F40	50	22	*POMT2*	+			+		+		+		+	
F41	51	23	*POMGNT1*			+	+					+		+
F42	52	21	*POMGNT1*			+	+					+		+
	53	22	*POMGNT1*			+		+				+		+
F43	54	27	*POMT1*	+			+		+		+		+	
F44	55	24	*POMGNT1*			+		+	+			+	+	
F45	56	25	*POMT1*	+			+		+		+			+
F46	57	23	*POMT1*	+			+		+		+			+
F47	58	22	*LARGE*		+		+				+			+
	59	23	*LARGE*		+		+			+	+			+
F48	60	15	*POMT2*	+			+			+	+		+	
F49	61	27	*POMT2*	+			+		+		NA	NA	NA	NA
F50	62	25		+			+		+		+			+
F51	63	24		+			+			+	NA	NA	NA	NA
F52	64	23	*POMT1*	+			+			+	NA	NA	NA	NA
F53	65	24	*POMGNT1*			+		+		+	NA	NA	NA	NA

NA = not available; + = present.

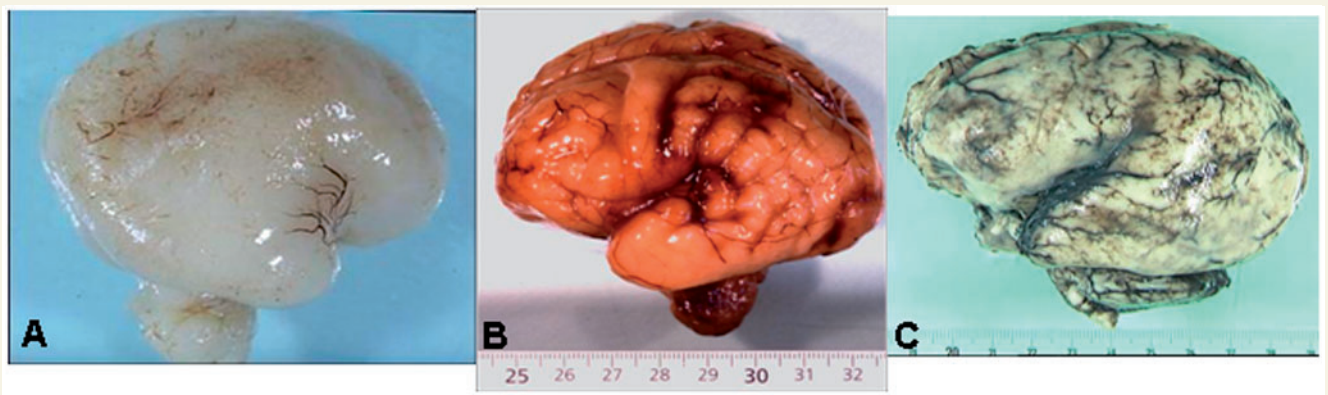

Figure 1 Appearance of the brain surface in cobblestone lissencephaly. (**A**) Cobblestone lissencephaly A at 19 weeks gestation. Note the lack of insular depression and the abnormal arachnoidal vessels. (**B**) Cobblestone lissencephaly C at 26 weeks gestation. Note poor sulcation and the irregular surface of the cerebral hemisphere, mainly of the frontal lobe. (**C**) Cobblestone lissencephaly A at 37 weeks gestation. Note total agyria of the hemisphere covered with whitish arachnoid with abnormal vascularization.

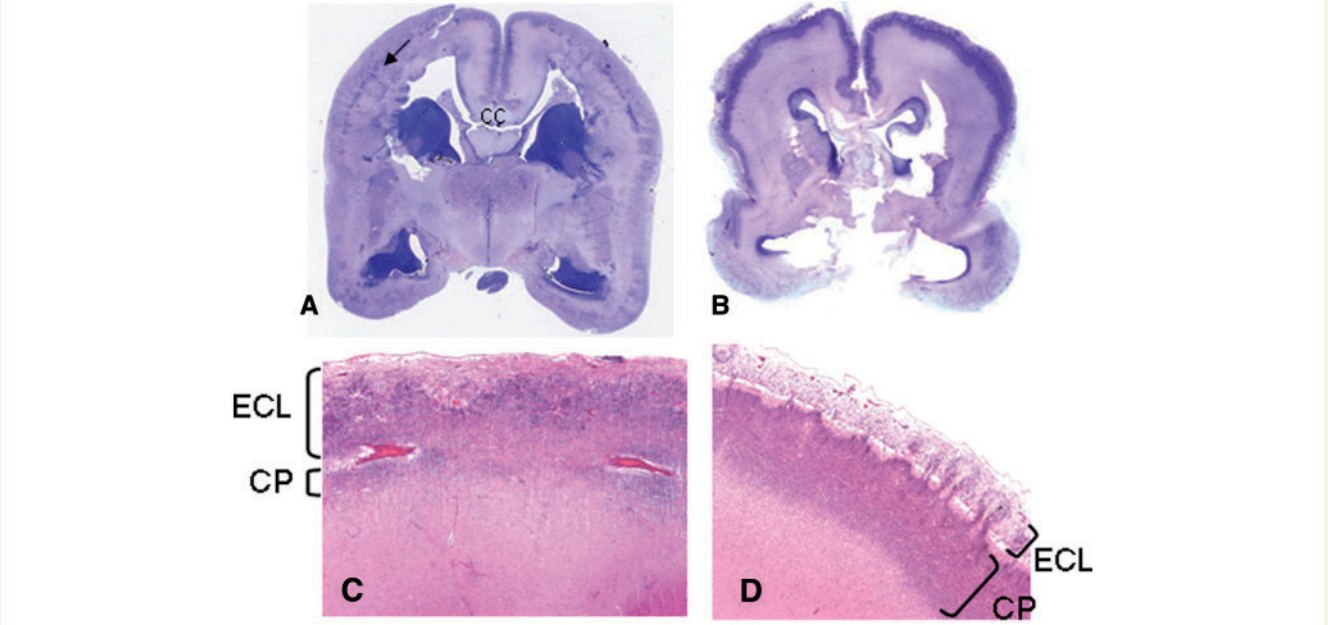

Figure 2 Whole-mount coronal sections of cerebral hemispheres in cobblestone lissencephaly A and cobblestone lissencephaly C stained with cresyl violet. (**A**) *POMT1* mutation at 19 weeks gestation. Note the severe cortical malformation leading to impoverishment of the cortical plate (arrow), unrecognizable at this magnification. Also note the ventricular enlargement and interdigitation of medial walls of dorsal telencephalon leading to the obstruction of the interhemispheric fissure. (**B**) *POMGNT1* mutation at 26 weeks gestation. Note the milder cortical malformation with a recognizable cortical ribbon under a thickened arachnoid. (**C**) Higher magnification of the frontoparietal cortex in cobblestone lissencephaly A showing the thick extracortical layer (ECL) and the thin residual cortical plate (CP). The interface between the extracortical layer and the residual cortical plate is marked by deepened arachnoidal vessels with tangential orientation. (**D**) Higher magnification of the frontoparietal cortex in cobblestone lissencephaly C, showing a thin extracortical layer above a well preserved cortical plate. CC = corpus callosum.

plates, leading to a fusion of cerebral walls and obstruction of the interhemispheric fissure (Fig. 2A), evocative on brain imaging of 'holoprosencephaly'. The existence of two dorsomedial hemispheric walls with two anterior cerebral arteries rules out the diagnosis of holoprosencephaly malformation. Basal ganglia were well developed. The brainstem and the cerebellum were severely affected. The cerebellum was hypoplastic and its foliation was abnormal (Fig. 3G). The fourth ventricle was enlarged. At the histological level, cerebellar dysplasia was always diffuse but variable in term of severity; major ($n = 33$) to minor ($n = 15$). Deep nuclei were disorganized. In this group, eyes available in 34 cases were asymmetrical in 13 cases. Retinal dysplasia varied from focal ($n = 2$) to diffuse ($n = 31$) and from major ($n = 11$) to minor ($n = 22$), ranging from total lack of lamination to foci of dysplasia. It was associated with cystic retinal coloboma ($n = 11$), cataract ($n = 11$) and anterior chamber synechia ($n = 9$). In one case retina were unremarkable on the examined levels.

Interestingly, neural tube defect and non-CNS malformations (facial clefts, visceral malformations and genital dysplasia) were found exclusively in this group. Skull defects ($n = 19$) concerned the occipital bone. Expressivity of neural tube defect was variable ranging from major occipital meningoencephalocele with double defects to minor meningocele. Equino varus foot deformations were present in 11 cases. Facial clefts were found in six cases and consisted of cleft lip/palate ($n = 2$), cleft palate ($n = 3$) and premaxillary agenesis ($n = 1$). Single or multiple visceral malformations were found in 24 foetuses, affecting kidneys, heart, lungs and the digestive tract. Kidney defects (hydronephrosis, renal dysplasia) were the most frequent ($n = 16$). Heart malformations (large ostium secundum, interventricular septal defect, pulmonary atresia or bicuspid aortic valves) were observed in five cases. Anal imperforation and/or intestinal malrotation were present in four cases. Abnormal pulmonary lobulation was noticed in four cases. Thymic agenesis was observed in one case. Gonadal dysgenesis affected either testis ($n = 9$) or ovaries ($n = 2$).

Cobblestone lissencephaly B

In 4/65 (6%) of foetuses aged from 22 to 27 weeks gestation, the extracortical layer/cortical plate ratio was variable, from negative to positive. The residual cortical plate was successively polymicrogyric, reduced to a fine rim or rather well organized. Ventricular dilatation was severe. The corpus callosum was abnormally thin in two cases (22 and 27 weeks gestation), thick in one case (23 weeks gestation) and not evaluable in the last case. Brainstem was severely affected as in cobblestone lissencephaly A. Cerebellum was small and malformed. At the histological level, cerebellar dysplasia was diffuse, but variable in terms of severity from major ($n = 2$) to minor ($n = 2$). Eyes evaluated in two cases showed no asymmetry but diffuse and minor retinal

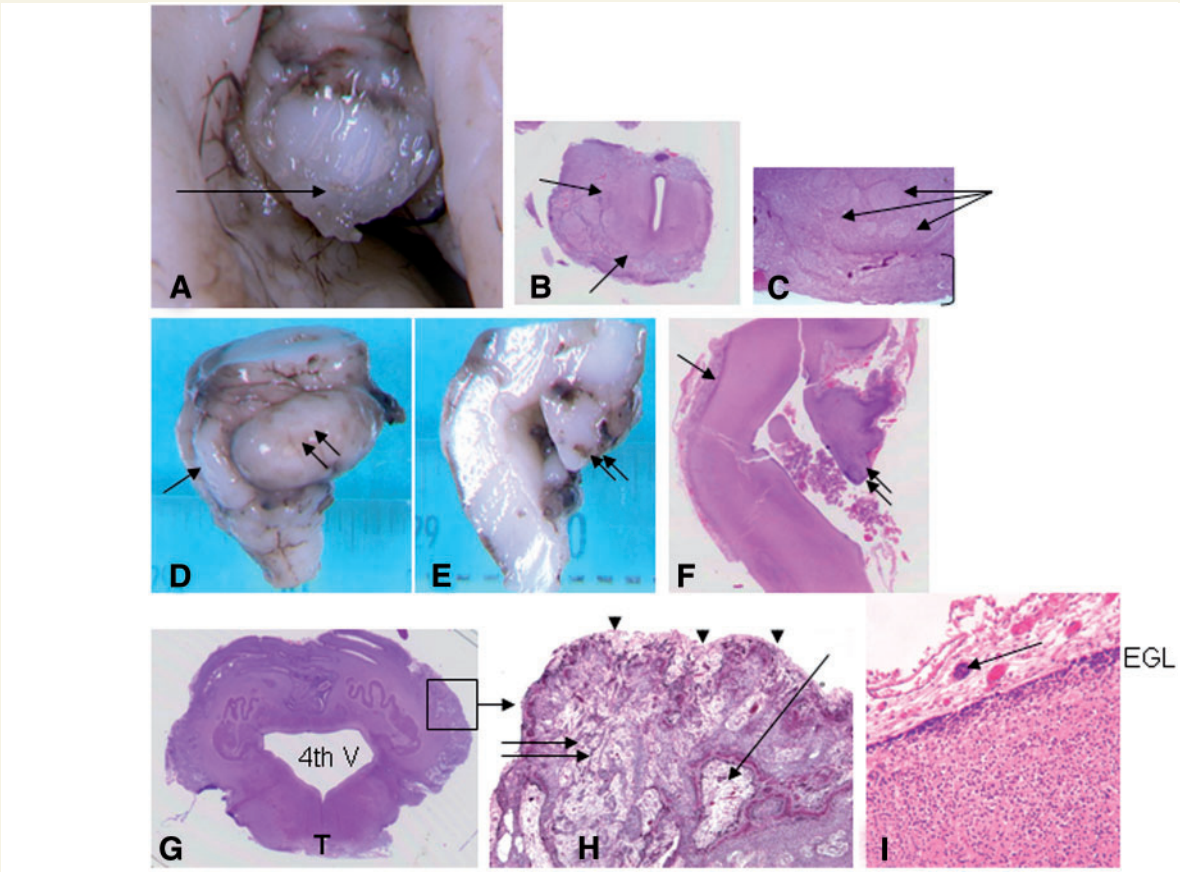

Figure 3 Brainstem and cerebellar anomalies in cobblestone lissencephaly. (**A**) Macroscopic view of the transverse section of the brainstem at the mesencephalon level (19 weeks gestation). Note the thick leptomeningeal sheet (arrow) around the hypoplastic cerebral peduncles. (**B**) Low magnification of the hypoplastic cerebral peduncles containing a dysmorphic aqueduct of Sylvius and surrounded by thickened leptomeninges (arrows). (**C**) High magnification of the peduncles containing bundles of disorganized fibres and tracts (arrows) and surrounded by thickened leptomeninges (bracket) filled with ectopic tracts. (**D**) Lateral view of the brainstem and cerebellum at 19 weeks gestation showing a flat pons (arrow) and poorly developed cerebellar hemisphere (double arrows). (**E**) Sagittal section of the brainstem and the cerebellum with (**F**) whole-mount histological preparation (haematoxylin and eosin), showing thick ventral leptomeninges (arrow), and a poorly developed vermis (double arrows). (**G**) Transverse section of the brainstem and the cerebellum (haematoxylin and eosin) showing dilated fourth ventricle (4th V), hypoplastic tegmentum (T), abnormal deep nuclei (nucleus dentate), lack of normal foliation and lamination, shown with a higher magnification in **H**. (**H**) Note the lacunar presentation of the cerebellum with fused folia. Lacunas contain arachnoid tissue (arrow) and are surrounded from outside-in by strates of granule cells and Purkinje cells or are devoid of any laminar organization (double arrows). Under the arachnoid (arrow heads), the external granular layer is poorly cellular, fragmented or devoid of granule cell. (**I**) High magnification of the cerebellar cortices shows the irregular external granule layer (EGL) with foci of ectopic cells in the surrounding leptomeninges (arrow).

dysplasia. Anterior chamber synechia was found in one case. Non-CNS malformations were absent.

Cobblestone lissencephaly C

In 13/65 cases (20%), aged from 18 to 32 weeks gestation, the extracortical layer/cortical plate ratio was negative. The neuroglial ectopia through small gaps of the pial–glial barrier was mild (Fig. 2B and D). The extracortical layer/cortical plate ratio was negative. The limit between the arachnoid space and the cerebral parenchyma was well defined, interrupted by sprouts of over-migrating cells (Fig. 2D). Brain surface was smooth or granular (Fig. 1B). Ventricular dilatation was variable from moderate to severe. The corpus callosum studied in 12 cases was normal in six (from 21 to 32 weeks gestation), thin in three cases (from 18 to 24 weeks gestation), and absent in three cases. Brainstem was severely affected, as in cobblestone lissencephaly A. Cerebellar foliation was partially disorganized and the fourth ventricle enlarged. At the histological level, cerebellar dysplasia was variable in terms of distribution, diffuse ($n = 6$) to focal ($n = 7$) often minor ($n = 11$) and rarely major ($n = 2$). In this group, eyes were asymmetrical in one case, but retinal dysplasia was found in six cases (out of seven examined). It was constantly focal, mainly minor (in five cases) and severe in one case. Limb anomalies were found in five cases. No other associated malformation was observed.

Molecular study

Pathogenic mutations were found in 43 cases (66%), in 36 unrelated families (68%). All together, we identified 45 distinct mutations, including 32 novel mutations (Supplementary material). Mutations involved the *POMT1* (22 cases/18 families), the *POMT2* (five cases/five families), the *POMGNT1* (12 cases/10 families), the *LARGE* (three cases/two families) and the *FKRP* (one case) genes, respectively. No mutation was found in *FKTN*. In 26 families, the affected individuals were compound heterozygote, whereas 10 patients were homozygote. In 22 foetuses (34%) born to 17 families (32%), no mutation was identified.

Phenotype–genotype correlations

Phenotype–genotype correlation studies (Table 3) correlate the most severe form (cobblestone lissencephaly A) to *POMT1* ($n = 22$), *POMT2* ($n = 5$) and *FKRP* ($n = 1$) gene mutations, while the least severe form (cobblestone lissencephaly C) was exclusively linked to *POMGNT1* ($n = 12$) gene mutations. The intermediate form (cobblestone lissencephaly B) was linked to mutations of the *LARGE* gene ($n = 3$). The 22 foetuses without any identified mutation, displayed a phenotype compatible with cobblestone lissencephaly A in 20 cases, with cobblestone lissencephaly B in one case and with cobblestone lissencephaly C in one case. Familial forms reoccurred with similar pattern for CNS anomalies, but displayed variable extracerebral abnormalities.

Discussion

CNS malformations are now exquisitely evaluated through brain imaging. However, neuropathological studies remain a valuable tool mainly in the context of cortical malformations. Our study in this series of 65 cases with cobblestone lissencephaly, selected on the basis of histoneuropathological criteria, shows the positive impact of neuropathology on the identification of α-dystroglycanopathies. After sequencing the genes of α-dystroglycanopathies, we observed a causal mutation in 66% of cases, while with neuroimaging criteria and biological values, mutations are found in 32–50% of patients. In addition, our study led us to the definition of a scoring system, useful for the evaluation of severity and permits phenotype/genotype correlations. Interestingly, our morphological classification showed to be helpful for the orientation of genetic screening of *POMT1*, *POMT2*, *POMGNT1*, *LARGE* and *FKRP*. Furthermore, our studies permit a better characterization and understanding of the neurodevelopmental processes underlying supratentorial and infratentorial anomalies in cobblestone lissencephaly.

Spectrum of cobblestone lissencephaly

Expressivity of α-dystroglycanopathies is variable and classically linked to the degree of dystroglycan hypoglycosylation. However, recent data suggest that severity depends also on the type of mutation (Brockington *et al.*, 2001*b*; D'Amico *et al.*, 2006; van Reeuwijk *et al.*, 2006; Godfrey *et al.*, 2007; Clement *et al.*, 2008; Messina *et al.*, 2008; Mercuri *et al.*, 2009). The most severe end of the spectrum of α-dystroglycanoapthies may be early embryonic lethality as supported by the mouse models of dystroglycan (Williamson *et al.*, 1997) and *FKRP* gene deficiency (Chan *et al.*, 2010). One can hypothesize that prenatal brain imaging permits identification of severe forms with early onset. Indeed, prenatal ultrasound screening permits identification of ventricular enlargement as early as 14 weeks gestation. However, diagnosis of agyria/pachygyria cannot be discussed before 22 weeks gestation, because of the physiologically smooth appearance of cerebral hemispheres. All index cases of our series were diagnosed after neuropathological investigation.

In our series, severe forms (cobblestone lissencephaly A) represent the majority of cases and concord with the Walker–Warburg Syndrome (van Reeuwijk *et al.*, 2005). Neural tube defects (occipital meningoencephalocele) and non-CNS malformations (facial clefts, visceral malformations and genital dysplasia) were found exclusively in this group. A causal mutation was identified in more than half of cases, involving *POMT1*, *POMT2* and *FKRP* ($n = 1$). Except one, all mutations found in *POMT1* and *POMT2* genes were truncated and presumably responsible for a severe deficit of α-dystroglycan glycosylation. POMT1, POMT2 are known to be involved in the first steps of *O*-glycosylation of α-dystroglycan and presumably responsible for a severe deficit of α-dystroglycan glycosylation (Takahashi *et al.*, 2001; Manya *et al.*, 2004; Akasaka-Manya *et al.*, 2006). Thus, the high prevalence of *POMT1* and the involvement of *POMT2* in our series of severe cobblestone lissencephaly are not surprising. However, these results are in contrast with some reports on post-natal cases, which found mutations in *POMT1* and *POMT2* genes diversely linked to severe and mild phenotypes (Beltran-Valero de Bernabe *et al.*, 2002; Muntoni *et al.*, 2007). Currier *et al*. (2005) found mutations of *POMT1* in only 2 of 30 patients with classic Walker–Warburg Syndrome and considered *POMT1* to be an uncommon cause of this syndrome. Of note, the association in our series of *FKRP* gene deficit with a severe phenotype, although found in one case, is unusual. Indeed, mutations in *FKRP* gene are classically found in muscular congenital dystrophies and limb girdle muscular dystrophy without brain involvement (Brockington *et al.*, 2001*a*, *b*; Esapa *et al.*, 2002, 2005). Our findings confirm the unusual association of *FKRP* mutations with Walker–Warburg syndrome and muscle–eye–brain phenotypes, previously documented in two unrelated patients (Beltran-Valero de Bernabe *et al.*, 2004). The function of FKRP is still unknown. It seems that FKRP is required for the post-translational modification of α-dystroglycan in the Golgi apparatus, which could be a novel mechanism that causes congenital muscular dystrophy (Esapa *et al.*, 2002).

In one-fifth of the cases (cobblestone lissencephaly C), the ratio between extracortical layer/cortical plate was negative. In addition, cerebellar dysplasia either diffuse or focal was mainly minor and retinal dysplasia was focal or absent. No neural tube defect or non-CNS associated malformations were found. This 'milder' phenotype is reminiscent of muscle–eye–brain syndrome, linked to the *POMGNT1* gene, which acts later on during *O*-glycosylation. Classically, muscle–eye–brain syndrome occurs in the neonatal period with severe muscle weakness and high serum creatine phosphokinase. Encephalocele is absent. Mental retardation and congenital myopia are usual. Cerebral anomalies are

Table 3 Phenotype/genotype correlation in the three subtypes of cobblestone lissencephaly

		Cobblestone lissencephaly A				Cobblestone lissencephaly B		Cobblestone lissencephaly C	
Genes	Total	*POMT1*	*POMT2*	*FKRP*	No mutation	*LARGE*	No mutation	*POMGNT1*	No mutation
Cases	65	22	5	1	20	3	1	12	1
Extracortical layer/cortical plate ratio	65								
Positive	48	22	5	1	20				
Variable	4					3	1		
Negative	13							12	1
Cerebellar dysplasia	65								
Diffuse	58	22	5	1	20	3	1	6	
Focal	7							6	1
Major	37	19	4		10	1	1	2	
Minor	28	3	1	1	10	2		10	1
Retinal dysplasia	41								
Diffuse	33	14	3	1	13	2			
Focal	8	1			1			6	
Major	12	3	3		5			1	
Minor	29	12		1	9	2		5	
Neural tube defect	19	6	1	0	12	0	0	0	0
Facial cleft	6	6	0	0	0	0	0	0	0
Micropenis	6	3	1	0	2	0	0	0	0
Gonadal dysgenesis	11	5	3	0	3	0	0	0	0
Visceral malformations	24	9	4	1	10	0	0	0	0

essentially reported on the basis of neuroimaging data. Neuropathological findings in muscle–eye–brain syndrome have been documented twice (Leyten *et al.*, 1991; Haltia *et al.*, 1997). Both highlight lack of cerebral cortical lamination and abnormal meninges with cerebellar disorganization, but with different degrees of severity. A severe phenotype reminiscent of a Walker–Warburg syndrome (Leyten *et al.*, 1991) could be opposed to a milder phenotype, close to Fukuyama cerebral and muscular dystrophy (Haltia *et al.*, 1997). In our series, all cases with cobblestone lissencephaly C, except one, were linked to *POMGNT1* gene mutations. Mutations in the *POMGNT1* gene were first identified in a Finnish population (Raitta *et al.*, 1978; Yoshida *et al.*, 2001), but have now been reported in different ethnic backgrounds (Taniguchi *et al.*, 2003). Since most of the affected families of our series were from French extraction, this confirms that *POMGNT1* mutations may be found in populations outside Finland, and that the clinical expressivity may be broader than recognized.

In a minority of the cases cobblestone lissencephaly B, the extracortical layer/cortical plate ratio was variable and the cortical plate was successively well organized or displayed a polymicrogyric pattern. The cerebellum was variably affected and the retinal dysplasia was diffuse, although minor. There was no associated malformation. In cobblestone lissencephaly B, mutations were exclusively found in the *LARGE* gene. The function of the *LARGE* gene is unknown but its over-expression restores *O*-glycosylation of α-dystroglycan in cells of patients with a *POMT1*, *POMGNT1*, *LARGE* or *FKTN* gene mutation (Barresi *et al.*, 2004). In our series, the small number of mutations in *LARGE* confirms the smaller involvement of this gene in α-dystroglycanopathies with brain involvement, as previously reported (van Reeuwijk *et al.*, 2007). Surprisingly, despite the large size of our series, no mutation was found in *FKTN* although this gene is known to be involved in Walker–Warburg syndrome, and considered to be the most common cause of this disease in the Middle East (Silan *et al.*, 2003; Cotarelo *et al.*, 2008; Manzini *et al.*, 2008). This discrepancy may be the result of our subjects being mainly from French extraction.

Pathogenesis and impact of glia limitans anomalies

In cobblestone lissencephaly, the underlying mechanism of cortical malformation is aberrant neuroglial ectopia within the arachnoid space, due to a defective interaction between radial glial progenitor cells and the outermost pial–glial membrane called 'glia limitans' (Ever and Gaiano, 2005). Studies have shown that integrity of the pial basement membrane is critical for the morphogenesis of the cerebral and cerebellar cortices (Hausmann and Sievers, 1985; Voss *et al.*, 2008).

The glia limitans is formed by the sixth week of development under the pia matter. It is composed of a meshwork of astrocytic processes covered by a distinct outer basal lamina. The basement membrane is produced by pial cells and remains in close contact with them (Zarbalis *et al.*, 2007). The endfeet of astrocytes are firmly attached to the basal lamina by junctional complexes, related to hemidesmosomes (Peters *et al.*, 1991). The integrity of glia limitans is crucial for the development of the cerebral cortex. By the sixth week of development, the primordial plexiform layer is set at the surface of cerebral hemispheres. Neurons of the plexiform layer, called Cajal–Retzius cells, are considered as

crucial in the cortical patterning. By the eighth week, waves of radial outward migration of neuroblasts along the radial glia, fed by the continued cell proliferation of the ventricular zone, lead to the formation of the highly organized cortical plate (Nadarajah and Parnavelas, 2002). Breaches in the basement membrane and/or in astrocytic endfeet lead to an overmigration of Cajal–Retzius cells into the arachnoid space and to an aberrant radial glia organization. This interferes with radial migration and results in an overmigration of post-mitotic neuroblasts into the arachnoid space and the formation of an extracortical layer, also containing Cajal–Retzius cells (F. Encha-Razavi, unpublished data). The overmigration of neuroglial precursors into the arachnoid space entails obstruction of the arachnoid space, contributing to cerebrospinal fluid retention. In the generation of ventricular dilatation, other factors such as reduction in cell numbers due to early damage to the ventricular zone may be also discussed. In addition, stenosis of the aqueduct and the complex hindbrain malformation may contribute to ventricular dilatation. In cobblestone lissencephaly, cortical malformations concord with disruption of the glia limitans (Bornemann *et al.*, 1996; Nakano *et al.*, 1996). The resulting extracortical layer is responsible for agyria or the cobblestone appearance of cerebral hemispheres. Limb malpositions are usually linked to muscular dystrophy. More likely, failure of generation of corticospinal tracts due to severe cortical malformation and/or their chaotic organization in the brainstem may cause arthrogryposis.

For a better characterization of infratentorial anomalies, the brainstem and the cerebellum were carefully analysed in our series. Of note, in all cases, the cerebellar leptomeninges contained irregular clusters of cells of granular morphology, while the Purkinje cells seemed to not be involved. Cerebellar granule cells are produced in the cerebellar anlage (rhombic lips) (Wang *et al.*, 2005; Fink *et al.*, 2006). They migrate rostrally and generate the external granular layer under the leptomeninges, in an anterior to posterior temporal gradient. Conversely, Purkinje cells are produced in the cerebellar ventricular zone and migrate radially into the cerebellar anlage, where they form a distinct layer under the external granular layer (Englund *et al.*, 2006; Fink *et al.*, 2006). Interaction between these two cell populations is crucial for proliferation of the granule cells and for normal cerebellar lamination (Wang and Zoghbi, 2001). In the cerebellum, the leptomeninges seem to be central for the migration of granule cells (Zarbalis *et al.*, 2007). They contribute to the formation of the cerebellar glia limitans, formed by glial endfeet (Bergmann glia), and are covered by a distinct basement membrane produced by pial cells. Interestingly, the cerebellum of mice lacking the gene for dystroglycan shows widespread discontinuities in the pial basement membrane and disruption of the glial scaffold with ectopic granule cells into the arachnoid space (Moore *et al.*, 2002). Similarly, in *Gpr5*$^{-}$ mice, the glia limitans is interrupted in multiple locations with glial process often extending outside the cerebellum (Koirala *et al.*, 2009). In addition, granule cells are present in ectopic locations outside the disrupted pial membrane. The interaction between granule cells and the basement membrane of the glia limitans seems to be central to granule cell migration. Faulty interaction results in abnormal migration of granule cells, responsible for abnormal positioning of all cell types. In the brainstem, rarefaction of pontine neurons and abnormal inferior olives may also be linked to a defect of the pial tangential pathway (Bornemann *et al.*, 1996; Nakano *et al.*, 1996). However, the impact of neuroglial ectopia and rarefaction of cerebellar projections may also be discussed.

The timing and mechanism of the defects in the glia limitans are under intensive study. Among potential causes, the inability of the pial–glial limiting membrane to grow in conjunction with growth of the brain is suggested (Koirala *et al.*, 2009). Indeed, mice with a *Foxc1* allele display detachment of radial glia endfeet, marginal zone heterotopias and cortical dyslamination (Zarbalis *et al.*, 2007; Hecht *et al.*, 2010). The authors conclude that these 'anomalies have some features resembling defects in type 2 (cobblestone) lissencephaly but appear later in corticogenesis because of the delay in breakdown of the basement membrane'. In our series, the cytoarchitecture of the cerebral hemispheres, the brainstem and the cerebellum was affected as early as 14–15 weeks gestation. A positive extracortical layer/cortical plate ratio (characteristic of severe forms) was found as early as 14–15 weeks gestation and up to 41 weeks gestation, while a negative extracortical layer/cortical plate ratio (characteristic of milder forms) was present later on during gestation, from 18 to 32 weeks.

The impact of the proteins encoded by the genes involved in abnormal *O*-glycosylation of α-dystroglycan on the basement membrane organization accounts for lesions observed in the brain and skeletal muscles (Takada *et al.*, 1984; Michele *et al.*, 2002; Ross, 2002; Jayasinha *et al.*, 2003; Chiyonobu *et al.*, 2005). We hypothesize that basement membrane anomalies may also be at the origin of facial clefts. Considering the skull defects, recent studies in mice suggest that they may be linked to a defective meningeal signalling, required for skull ossification (Zarbalis *et al.*, 2007).

Cobblestone lissencephaly is highly evocative of α-dystroglycanopathies. Most of the genes associated with these disorders are associated with abnormal glycosylation of α-dystroglycan. However, despite our intensive molecular screening, a third of cases with cobblestone lissencephaly remained unexplained suggesting that other genes and/or pathways may be involved. Recently, haploinsufficiency of the dystroglycan gene itself (Frost *et al.*, 2010) and mutation in *SRD5A3*, a gene involved in dolichol metabolism, have been reported in relation with muscle–eye–brain/Walker–Warburg phenotypes (Satz *et al.*, 2008; Frost *et al.*, 2010; Morava *et al.* 2010). In addition, heterozygous missense mutations in the *COL4A1* gene have been found in relation with two cases described as compatible with muscle–eye–brain/Walker–Warburg phenotypes (Labelle-Dumais *et al.*, 2011). In murine models, 'cobblestone-like' disorders have been found associated with defects in the pial basement membrane and abnormal anchorage of the radial glial cell endfeet (Li *et al.*, 2008). In addition, polymicrogyria associated with some neuroglial ectopia and cerebellar anomalies have been documented in a foetus with mutation in *GPR56* (Bahi-Buisson *et al.*, 2010).

We conclude that cobblestone lissencephaly encompasses a spectrum of cortical anomalies with at least three subtypes, regardless of age and with good genetic correlations. In the cerebellum, histopathological changes support a novel hypothesis that

the cerebellar defects arise from the disrupted adhesion of developing granule cells to the pial basement membrane. Our findings offer a rich research perspective for a better understanding of neurodevelopmental processes affected in cobblestone lissencephaly and for the identification of other pathogenic pathways and/or responsible gene(s).

Acknowledgements

We are grateful to Prof. Michel Vekemans, University Paris Descartes, Hôpital Necker-Enfants malades for his critical reading of our article.

Funding

The Assistance Publique-Hôpitaux de Paris (CIRC 04149); the Société Française de Fœtopathologie (SOFFOET).

Supplementary material

Supplementary material is available at *Brain* online.

References

Akasaka-Manya K, Manya H, Nakajima A, Kawakita M, Endo T. Physical and functional association of human protein o-mannosyltransferases 1 and 2. J Biol Chem 2006; 281: 19339–45.

Bahi-Buisson N, Poirier K, Boddaert N, Fallet-Bianco C, Specchio N, Bertini E, et al. GPR56-related bilateral frontoparietal polymicrogyria: further evidence for an overlap with the cobblestone complex. Brain 2010; 133: 3194–209.

Barkovich AJ. Neuroimaging manifestations and classification of congenital muscular dystrophies. AJNR Am J Neuroradiol 1998; 19: 1389–96.

Barkovich AJ, Kuzniecky RI, Jackson GD, Guerrini R, Dobyns WB. Classification system for malformations of cortical development: update 2001. Neurology 2001; 57: 2168–78.

Barkovich AJ, Kuzniecky RI, Jackson GD, Guerrini R, Dobyns WB. A developmental and genetic classification for malformations of cortical development. Neurology 2005; 65: 1873–87.

Barresi R, Campbell KP. Dystroglycan: from biosynthesis to pathogenesis of human disease. J Cell Sci 2006; 119 (Pt 2): 199–207.

Barresi R, Michele DE, Kanagawa M, Harper HA, Dovico SA, Satz JS, et al. LARGE can functionally bypass alpha-dystroglycan glycosylation defects in distinct congenital muscular dystrophies. Nat Med 2004; 10: 696–703.

Beltran-Valero de Bernabe D, Currier S, Steinbrecher A, Celli J, van Beusekom E, van der Zwaag B, et al. Mutations in the O-mannosyltransferase gene POMT1 give rise to the severe neuronal migration disorder Walker-Warburg syndrome. Am J Hum Genet 2002; 71: 1033–43.

Beltran-Valero de Bernabe D, Voit T, Longman C, Steinbrecher A, Straub V, Yuva Y, et al. Mutations in the FKRP gene can cause muscle-eye-brain disease and Walker-Warburg syndrome. J Med Genet 2004; 41: e61.

Bornemann A, Pfeiffer R, Beinder E, Wenkel H, Schlicker U, Meyermann R, et al. Three siblings with Walker-Warburg Syndrome. Gen Diagn Pathol 1996; 141: 371–5.

Bouchet C, Gonzales M, Vuillaumier-Barrot S, Devisme L, Lebizec C, Alanio E, et al. Molecular heterogeneity in fetal forms of type II lissencephaly. Hum Mutat 2007; 28: 1020–7.

Brockington M, Blake DJ, Prandini P, Brown SC, Torelli S, Benson MA, et al. Mutations in the fukutin-related protein gene (FKRP) cause a form of congenital muscular dystrophy with secondary laminin alpha2 deficiency and abnormal glycosylation of alpha-dystroglycan. Am J Hum Genet 2001a; 69: 1198–209.

Brockington M, Yuva Y, Prandini P, Brown SC, Torelli S, Benson MA, et al. Mutations in the fukutin-related protein gene (FKRP) identify limb girdle muscular dystrophy 2I as a milder allelic variant of congenital muscular dystrophy MDC1C. Hum Mol Genet 2001b; 10: 2851–9.

Chan YM, Keramaris-Vrantsis E, Lidov HG, Norton JH, Zinchenko N, Gruber HE, et al. Fukutin-related protein is essential for mouse muscle, brain and eye development and mutation recapitulates the wide clinical spectrums of dystroglycanopathies. Hum Mol Genet 2010; 19: 3995–4006.

Chiyonobu T, Sasaki J, Nagai Y, Takeda S, Funakoshi H, Nakamura T, et al. Effects of fukutin deficiency in the developing mouse brain. Neuromuscul Disord 2005; 15: 416–26.

Clement EM, Godfrey C, Tan J, Brockington M, Torelli S, Feng L, et al. Mild POMGnT1 mutations underlie a novel limb-girdle muscular dystrophy variant. Arch Neurol 2008; 65: 137–41.

Cotarelo RP, Valero MC, Prados B, Pena A, Rodriguez L, Fano O, et al. Two new patients bearing mutations in the fukutin gene confirm the relevance of this gene in Walker-Warburg syndrome. Clin Genet 2008; 73: 139–45.

Currier SC, Lee CK, Chang BS, Bodell AL, Pai GS, Job L, et al. Mutations in POMT1 are found in a minority of patients with Walker-Warburg syndrome. Am J Med Genet A 2005; 133A: 53–7.

D'Amico A, Tessa A, Bruno C, Petrini S, Biancheri R, Pane M, et al. Expanding the clinical spectrum of POMT1 phenotype. Neurology 2006; 66: 1564–7, discussion 461.

Dambska M, Wisniewski K, Sher JH. Lissencephaly: two distinct clinico-pathological types. Brain Dev 1983; 5: 302–10.

Dobyns WB, Pagon RA, Armstrong D, Curry CJ, Greenberg F, Grix A, et al. Diagnostic criteria for Walker-Warburg syndrome. Am J Med Genet 1989; 32: 195–210.

Encha-Razavi F, Chelly J. Pitfalls of the morphologic approach. J Neuropathol Exp Neurol 2006; 65: 302, author reply 303.

Englund C, Kowalczyk T, Daza RA, Dagan A, Lau C, Rose MF, et al. Unipolar brush cells of the cerebellum are produced in the rhombic lip and migrate through developing white matter. J Neurosci 2006; 26: 9184–95.

Esapa CT, Benson MA, Schroder JE, Martin-Rendon E, Brockington M, Brown SC, et al. Functional requirements for fukutin-related protein in the Golgi apparatus. Hum Mol Genet 2002; 11: 3319–31.

Esapa CT, McIlhinney RA, Blake DJ. Fukutin-related protein mutations that cause congenital muscular dystrophy result in ER-retention of the mutant protein in cultured cells. Hum Mol Genet 2005; 14: 295–305.

Ever L, Gaiano N. Radial 'glial' progenitors: neurogenesis and signaling. Curr Opin Neurobiol 2005; 15: 29–33.

Fink AJ, Englund C, Daza RA, Pham D, Lau C, Nivison M, et al. Development of the deep cerebellar nuclei: transcription factors and cell migration from the rhombic lip. J Neurosci 2006; 26: 3066–76.

Frost AR, Bohm SV, Sewduth RN, Josifova D, Ogilvie CM, Izatt L, et al. Heterozygous deletion of a 2-Mb region including the dystroglycan gene in a patient with mild myopathy, facial hypotonia, oral-motor dyspraxia and white matter abnormalities. Eur J Hum Genet 2010; 18: 852–5.

Fukuyama Y, Osawa M, Suzuki H. Congenital progressive muscular dystrophy of the Fukuyama type - clinical, genetic and pathological considerations. Brain Dev 1981; 3: 1–29.

Godfrey C, Clement E, Mein R, Brockington M, Smith J, Talim B, et al. Refining genotype phenotype correlations in muscular dystrophies with defective glycosylation of dystroglycan. Brain 2007; 130 (Pt 10): 2725–35.

Haltia M, Leivo I, Somer H, Pihko H, Paetau A, Kivela T, et al. Muscle-eye-brain disease: a neuropathological study. Ann Neurol 1997; 41: 173–80.

Hausmann B, Sievers J. Cerebellar external granule cells are attached to the basal lamina from the onset of migration up to the end of their proliferative activity. J Comp Neurol 1985; 241: 50–62.
Hecht JH, Siegenthaler JA, Patterson KP, Pleasure SJ. Primary cellular meningeal defects cause neocortical dysplasia and dyslamination. Ann Neurol 2010; 68: 454–64.
Jayasinha V, Nguyen HH, Xia B, Kammesheidt A, Hoyte K, Martin PT. Inhibition of dystroglycan cleavage causes muscular dystrophy in transgenic mice. Neuromuscul Disord 2003; 13: 365–75.
Jellinger K, Rett A. Agyria-pachygyria (lissencephaly syndrome). Neuropadiatrie 1976; 7: 66–91.
Jissendi-Tchofo P, Kara S, Barkovich AJ. Midbrain-hindbrain involvement in lissencephalies. Neurology 2009; 72: 410–8.
Koirala S, Jin Z, Piao X, Corfas G. GPR56-regulated granule cell adhesion is essential for rostral cerebellar development. J Neurosci 2009; 29: 7439–49.
Labelle-Dumais C, Dilworth DJ, Harrington EP, de Leau M, Lyons D, Kabaeva Z, et al. COL4A1 mutations cause ocular dysgenesis, neuronal localization defects, and myopathy in mice and Walker-Warburg syndrome in humans. PLoS Genet 2011; 7: e1002062.
Leyten QH, Renkawek K, Renier WO, Gabreels FJ, Mooy CM, ter Laak HJ, et al. Neuropathological findings in muscle-eye-brain disease (MEB-D). Neuropathological delineation of MEB-D from congenital muscular dystrophy of the Fukuyama type. Acta Neuropathol 1991; 83: 55–60.
Li S, Jin Z, Koirala S, Bu L, Xu L, Hynes RO, et al. GPR56 regulates pial basement membrane integrity and cortical lamination. J Neurosci 2008; 28: 5817–26.
Manya H, Chiba A, Yoshida A, Wang X, Chiba Y, Jigami Y, et al. Demonstration of mammalian protein O-mannosyltransferase activity: coexpression of POMT1 and POMT2 required for enzymatic activity. Proc Natl Acad Sci USA 2004; 101: 500–5.
Manzini MC, Gleason D, Chang BS, Hill RS, Barry BJ, Partlow JN, et al. Ethnically diverse causes of Walker-Warburg syndrome (WWS): FCMD mutations are a more common cause of WWS outside of the Middle East. Hum Mutat 2008; 29: E231–41.
Mercuri E, Messina S, Bruno C, Mora M, Pegoraro E, Comi GP, et al. Congenital muscular dystrophies with defective glycosylation of dystroglycan: a population study. Neurology 2009; 72: 1802–9.
Messina S, Mora M, Pegoraro E, Pini A, Mongini T, D'Amico A, et al. POMT1 and POMT2 mutations in CMD patients: a multicentric Italian study. Neuromuscul Disord 2008; 18: 565–71.
Michele DE, Barresi R, Kanagawa M, Saito F, Cohn RD, Satz JS, et al. Post-translational disruption of dystroglycan-ligand interactions in congenital muscular dystrophies. Nature 2002; 418: 417–22.
Moore SA, Saito F, Chen J, Michele DE, Henry MD, Messing A, et al. Deletion of brain dystroglycan recapitulates aspects of congenital muscular dystrophy. Nature 2002; 418: 422–5.
Morava E, Kuhnisch J, Drijvers JM, Robben JH, Cremers C, van Setten P, et al. Autosomal recessive mental retardation, deafness, ankylosis, and mild hypophosphatemia associated with a novel ANKH mutation in a consanguineous family. J Clin Endocrinol Metab 2010; 96: E189–98.
Muntoni F, Brockington M, Godfrey C, Ackroyd M, Robb S, Manzur A, et al. Muscular dystrophies due to defective glycosylation of dystroglycan. Acta Myol 2007; 26: 129–35.
Nadarajah B, Parnavelas JG. Modes of neuronal migration in the developing cerebral cortex. Nat Rev Neurosci 2002; 3: 423–32.
Nakano I, Funahashi M, Takada K, Toda T. Are breaches in the glia limitans the primary cause of the micropolygyria in Fukuyama-type congenital muscular dystrophy (FCMD)? Pathological study of the cerebral cortex of an FCMD fetus. Acta Neuropathol 1996; 91: 313–21.
Pagon RA, Chandler JW, Collie WR, Clarren SK, Moon J, Minkin SA, et al. Hydrocephalus, agyria, retinal dysplasia, encephalocele (HARD +/− E) syndrome: an autosomal recessive condition. Birth Defects Orig Artic Ser 1978; 14: 233–41.
Peters A, Palay SL, Webster H. The fine structure of the nervous system: neurons and their supporting cells. New York: Oxford University Press; 1991.
Raitta C, Lamminen M, Santavuori P, Leisti J. Ophthalmological findings in a new syndrome with muscle, eye and brain involvement. Acta Ophthalmol (Copenh) 1978; 56: 465–72.
Ross ME. Full circle to cobbled brain. Nature 2002; 418: 376–7.
Santavuori P, Somer H, Sainio K, Rapola J, Kruus S, Nikitin T, et al. Muscle-eye-brain disease (MEB). Brain Dev 1989; 11: 147–53.
Satz JS, Barresi R, Durbeej M, Willer T, Turner A, Moore SA, et al. Brain and eye malformations resembling Walker-Warburg syndrome are recapitulated in mice by dystroglycan deletion in the epiblast. J Neurosci 2008; 28: 10567–75.
Silan F, Yoshioka M, Kobayashi K, Simsek E, Tunc M, Alper M, et al. A new mutation of the fukutin gene in a non-Japanese patient. Ann Neurol 2003; 53: 392–6.
Takada K, Nakamura H, Tanaka J. Cortical dysplasia in congenital muscular dystrophy with central nervous system involvement (Fukuyama type). J Neuropathol Exp Neurol 1984; 43: 395–407.
Takahashi S, Sasaki T, Manya H, Chiba Y, Yoshida A, Mizuno M, et al. A new beta-1,2-N-acetylglucosaminyltransferase that may play a role in the biosynthesis of mammalian O-mannosyl glycans. Glycobiology 2001; 11: 37–45.
Taniguchi K, Kobayashi K, Saito K, Yamanouchi H, Ohnuma A, Hayashi YK, et al. Worldwide distribution and broader clinical spectrum of muscle-eye-brain disease. Hum Mol Genet 2003; 12: 527–34.
van der Knaap MS, Smit LM, Barth PG, Catsman-Berrevoets CE, Brouwer OF, Begeer JH, et al. Magnetic resonance imaging in classification of congenital muscular dystrophies with brain abnormalities. Ann Neurol 1997; 42: 50–9.
van Reeuwijk J, Brunner HG, van Bokhoven H. Glyc-O-genetics of Walker-Warburg syndrome. Clin Genet 2005; 67: 281–9.
van Reeuwijk J, Maugenre S, van den Elzen C, Verrips A, Bertini E, Muntoni F, et al. The expanding phenotype of POMT1 mutations: from Walker-Warburg syndrome to congenital muscular dystrophy, microcephaly, and mental retardation. Hum Mutat 2006; 27: 453–9.
van Reeuwijk J, Grewal PK, Salih MA, Beltran-Valero de Bernabe D, McLaughlan JM, Michielse CB, et al. Intragenic deletion in the LARGE gene causes Walker-Warburg syndrome. Hum Genet 2007; 121: 685–90.
Viot G, Sonigo P, Simon I, Simon-Bouy B, Chadeyron F, Beldjord C, et al. Neocortical neuronal arrangement in LIS1 and DCX lissencephaly may be different. Am J Med Genet A 2004; 126A: 123–8.
Voss AK, Britto JM, Dixon MP, Sheikh BN, Collin C, Tan SS, et al. C3G regulates cortical neuron migration, preplate splitting and radial glial cell attachment. Development 2008; 135: 2139–49.
Wang VY, Rose MF, Zoghbi HY. Math1 expression redefines the rhombic lip derivatives and reveals novel lineages within the brainstem and cerebellum. Neuron 2005; 48: 31–43.
Wang VY, Zoghbi HY. Genetic regulation of cerebellar development. Nat Rev Neurosci 2001; 2: 484–91.
Williamson RA, Henry MD, Daniels KJ, Hrstka RF, Lee JC, Sunada Y, et al. Dystroglycan is essential for early embryonic development: disruption of Reichert's membrane in Dag1-null mice. Hum Mol Genet 1997; 6: 831–41.
Yoshida A, Kobayashi K, Manya H, Taniguchi K, Kano H, Mizuno M, et al. Muscular dystrophy and neuronal migration disorder caused by mutations in a glycosyltransferase, POMGnT1. Dev Cell 2001; 1: 717–24.
Zarbalis K, Siegenthaler JA, Choe Y, May SR, Peterson AS, Pleasure SJ. Cortical dysplasia and skull defects in mice with a Foxc1 allele reveal the role of meningeal differentiation in regulating cortical development. Proc Natl Acad Sci USA 2007; 104: 14002–7.